The hydrography and dynamics of the ocean environment of the Prince Edward Islands (Southern Ocean)

I.J. Ansorge*, J.R.E. Lutjeharms

Department of Oceanography, University of Cape Town, 7700 Rondebosch, South Africa

Abstract

The Prince Edward Islands lie in the Indian sector of the Southern Ocean at 47°S and 38°E. They lie in the path of the Antarctic Circumpolar Current (ACC), between the Subantarctic Front (SAF) to the north and the Antarctic Polar Front (APF) to the south. Two extensive hydrographic surveys (MOES 2 and MIOS 2) have been carried out to establish for the first time the mesoscale hydrography and dynamics of the oceanic surroundings of these islands.

During the MOES 2, the SAF was deflected northward around the islands, while the APF lay south of the survey grid and south of the islands. Water masses in the region changed gradually from Subantarctic Surface Water (SASW) to Antarctic Surface Water (AASW) on crossing the Polar Frontal Zone (PFZ). Downstream of the islands, a wake, resulting in the generation of broad meanders, was formed. As a consequence, water masses, in particular warm SASW, were displaced from north of the SAF across the PFZ, while cooler waters, which have been modified in the transitional band of the PFZ, were displaced northwards.

In contrast, during MIOS 2, the surface expression of the SAF formed an intensive frontal band. On approaching the islands, the SAF split into two branches, with a branch deflected northwards around the islands, while a second branch meandered southward. In the downstream region, an intense cold eddy consisting of AASW was observed within the PFZ, displacing the SAF northwards. South of this eddy, a warm patch of SASW water was encountered, its position possibly controlled by the meandering SAF.

Evidence from both these surveys demonstrates that the ACC exhibits high degrees of mesoscale variability in the vicinity of the Prince Edward Islands. The displacement of the SAF in both instances was apparent, resulting in the advection or the entrapment of neighbouring water masses into and across the PFZ. The speed of the incident current on approaching the islands may play a role in the degree of mesoscale mixing downstream of the islands.
© 2002 Elsevier Science B.V. All rights reserved.

Keywords: Prince Edward Islands; Subantarctic Front; Polar Front Zone; Mesoscale disturbances; Frontal displacement

1. Introduction

The Prince Edward Islands, consisting of Marion and Prince Edward, lie east of the Southwest Indian Ridge and southwest of the Del Cano Rise (Fig. 1). The islands are volcanic outcrops approximately

* Corresponding author. Tel.: +27-21-650-3280; fax: +27-21-650-3979.
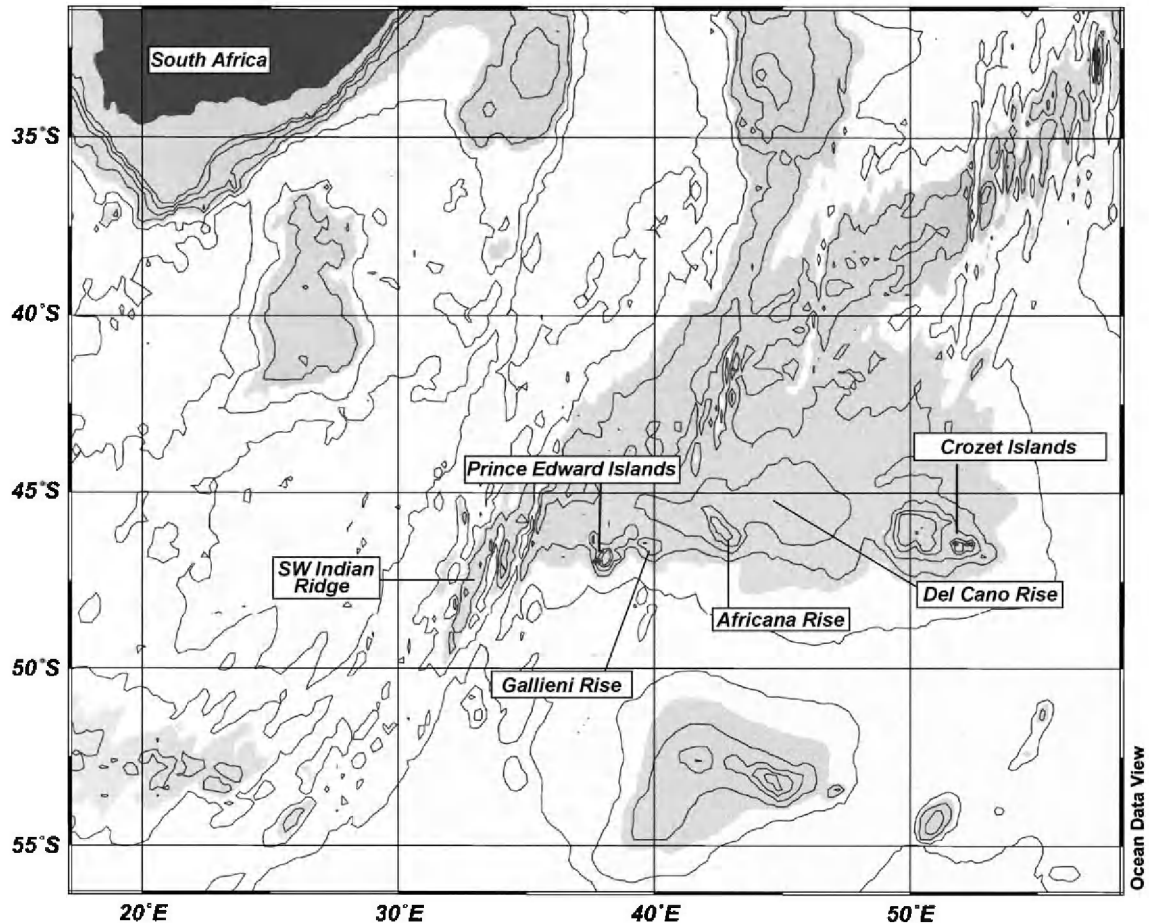E-mail address: ansorge@physci.uct.ac.za (I.J. Ansorge).

Fig. 1. Geographic location of the Prince Edward Islands in relation to southern Africa and the Crozet Islands. Lines represent isobaths for every 500 m.

250 000 years old (McDougal, 1971). Marion Island is the larger of the two (over 270 km^2), while Prince Edward Island, which lies 19 km to the northeast, covers approximately 45 km^2. A shallow saddle separates the islands, which is between 40 and 200 m deep. The islands rise steeply from a region of complex bottom topography and constitute an isolated surface feature. The nearest landfall is the Crozet Islands, 950 km to the east; South Africa is over 2000 km to the northwest (Fig. 1).

Intensive investigations carried out on the oceanic frontal systems south of Africa (Lutjeharms and Valentine, 1984; Duncombe Rae, 1989a,b; Belkin and Gordon, 1996) have shown that the Prince Edward Islands lie directly in the path of the Antarctic Circum-

polar Current (ACC), within the Polar Frontal Zone (PFZ). It has been shown that the northern and southern boundaries of the PFZ, represented by the Subantarctic (SAF) and Antarctic Polar Fronts (APF), exhibit high degrees of latitudinal variability in this region (Lutjeharms and Valentine, 1984; Lutjeharms, 1990; Duncombe Rae, 1989a,b; Belkin and Gordon, 1996). The meandering positions of the SAF and APF may play a crucial role in forming the macro- and mesoscale oceanographic environment of the islands.

The transport within the ACC is concentrated at the high-speed cores of the SAF and APF. The PFZ, a region of weaker geostrophic flow, separates these two frontal systems (Nowlin et al., 1977). When the SAF lies farther to the north, the PFZ is

broader and advective forces, associated with this relative quiescent zone, may be particularly weak. On such occasions, eddies have been observed over the shelf between Prince Edward and Marion Island (Perissinotto and Duncombe Rae, 1990; Pakhomov et al., 2000). Such eddies, if trapped, would protract the residence time of water masses on the interisland shelf; otherwise, these waters may move rapidly downstream. By contrast, when the SAF lies in close proximity to the islands, the stronger currents associated with the front prevail and eddies have in general not been found in the interisland region (Perissinotto et al., 2000; Ansorge et al., 1999; Pakhomov et al., 2000).

Intrusions of Subantarctic as well as Antarctic waters into the PFZ could conceivably take place during both these scenarios of incident flow. This would be consistent with the observed presence of planktonic species characteristic of both these regions at the islands (Boden and Parker, 1986). The processes responsible for such flow complexity could be the heterogeneous bottom topography of the region as well as the obstruction caused by the islands themselves.

Despite a large number of hydrographic surveys in the vicinity of the islands (Miller, 1982; Miller et al., 1984; Allanson et al., 1985; Boden and Parker, 1986; Boden, 1988; Duncombe Rae, 1989a,b; Perissinotto and Boden, 1989; Perissinotto and Duncombe Rae, 1990), only the shelf region between the two islands has been studied in detail. To try and resolve the influence of the SAF and the APF on the environment of the Prince Edward Islands and to place this impact in a broader geographic perspective, two extensive cruises were designed; they were the Marion Offshore Ecological Study 2 (MOES 2) in 1989 and a repeat cruise, the Marion Island Oceanographic Survey 2 (MIOS 2), in 1997.

2. Methods and materials

The two surveys were carried out in the upstream as well as the downstream regions of the Prince Edward Islands. Both the MOES 2 (Fig. 2a) and the MIOS 2 (Fig. 2b) were conducted during the early austral autumn. The MOES 2 was carried out in April 1989 and consisted of a grid of eight north–south

sections across the PFZ between 46°S and 47°30′S and between 35°51′E and 40°28′E (Fig. 2a). There were three lines upstream of the islands between 35°51′E and 37°07′E, four downstream between 38°27′E and 40°28′E, and one line extending approximately 180 nautical miles along the longitude on which the islands lie (37°48′E). Each line consisted of six alternate Conductivity–Temperature–Depth (CTD) and Expendable Bathythermograph (XBT) stations occupied at 16 nautical mile intervals.

The MIOS 2 (Fig. 2b) was designed as a comparative study, hence the survey grid consisted of similar transects as that of MOES 2, with alternate CTD and XBT stations on average 15 nautical miles apart. It was completed in April of 1997. In order to increase the spatial coverage of the PFZ, hydrographic transects extended farther south between 46° and 48°S and farther east between 36°10′ and 42°00′E than for the MOES 2. A total of 93 hydrographic stations were occupied in the region upstream, within the interisland region and downstream of the islands. Unfortunately, due to stormy conditions, the southernmost stations along transects 3 and 4 were missed and only repeated 3 days later as CTD 54 and 55 (Fig. 2b).

Vertical profiles were obtained at CTD stations using a Neil Brown Instruments system with a Mark IIIb underwater unit during MOES 2 (Van Ballegooyen et al., 1990) and a Mark IIIc upgrade during MIOS 2 (Ansorge et al., 1998). Unfortunately, oxygen samples were not collected during the MOES 2 survey and therefore only comparisons between Θ/S profiles can be made.

Sippican T7 XBTs were deployed to a maximum depth of 760 m. The probes were calibrated against water temperatures of the sea surface obtained with a Crawford bucket (Crawford, 1972). Each probe was placed in a water bath for 5 min before deployment in order to minimise the difference between the probe's storage temperature and that of the sea surface. In addition, a joint observation during MIOS 2 was undertaken at station 38 (48°S, 39°30′E) in order to compare the difference in temperature profiles between XBT and CTD probes. A difference of 0.1 °C was obtained (Ansorge et al., 1998).

Horizontal distributions for temperature and density (Figs. 4–7) were plotted using the kriging method used in the contouring package Surfer (v6.02) by
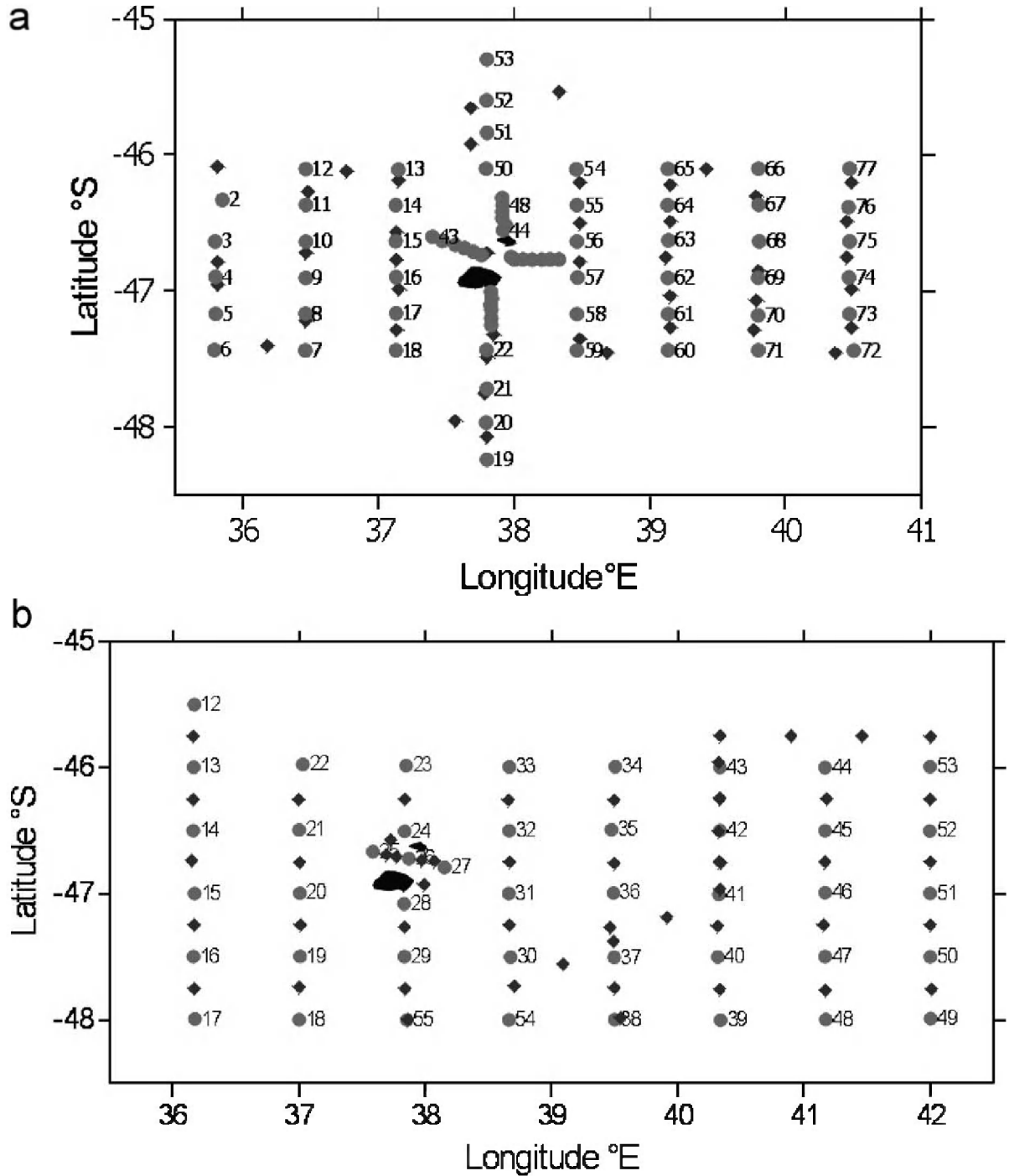
Fig. 2. Distribution of hydrographic stations occupied during the (a) MOES 2 and (b) MIOS 2 cruises in the oceanic environment of the Prince Edward Islands. CTD stations are shown as circles whereas XBT stations are diamonds. The Prince Edward Islands are marked in black.

Table 1
Definitions for the surface and subsurface expressions of the Subantarctic and Antarctic Polar Fronts

	Property range	Reference
Surface		
SAF	$T-S_0$ ranges of 6.3–9.7 °C and 33.85–33.94	Holliday and Read (1998)
APF	Maximum gradient of SST regime between 2 and 6 °C	Sparrow et al. (1995)
Subsurface		
SAF	$T-S_{200}$ ranges of 4.8–8.4 °C and 34.11–34.47 with axial values of 6.6 °C and 34.3	Belkin and Gordon (1996)
APF	Axial T_{200} is 2 °C	Orsi et al. (1995)

Golden Software. Grid limits and grid densities varied for each survey as a result of hydrographic transects during MIOS 2 extending further south between 46°

and 48°S and farther east between 36°10′ and 42°E than for MOES 2. In addition, contours in the grid files have been automatically smoothed in order to eliminate angular contours and to prevent the contouring of additional bulls eyes.

3. Identification of fronts and water masses

Identification of the main ACC fronts is essential in order to trace the upper level circulation associated with the baroclinic shear. However, accurate identification of the fronts is not always simple, especially in regions where they remain merged (Read and Pollard, 1983; Park et al., 1993). One major difficulty is the various definitions that have been given for the characterisation of the fronts
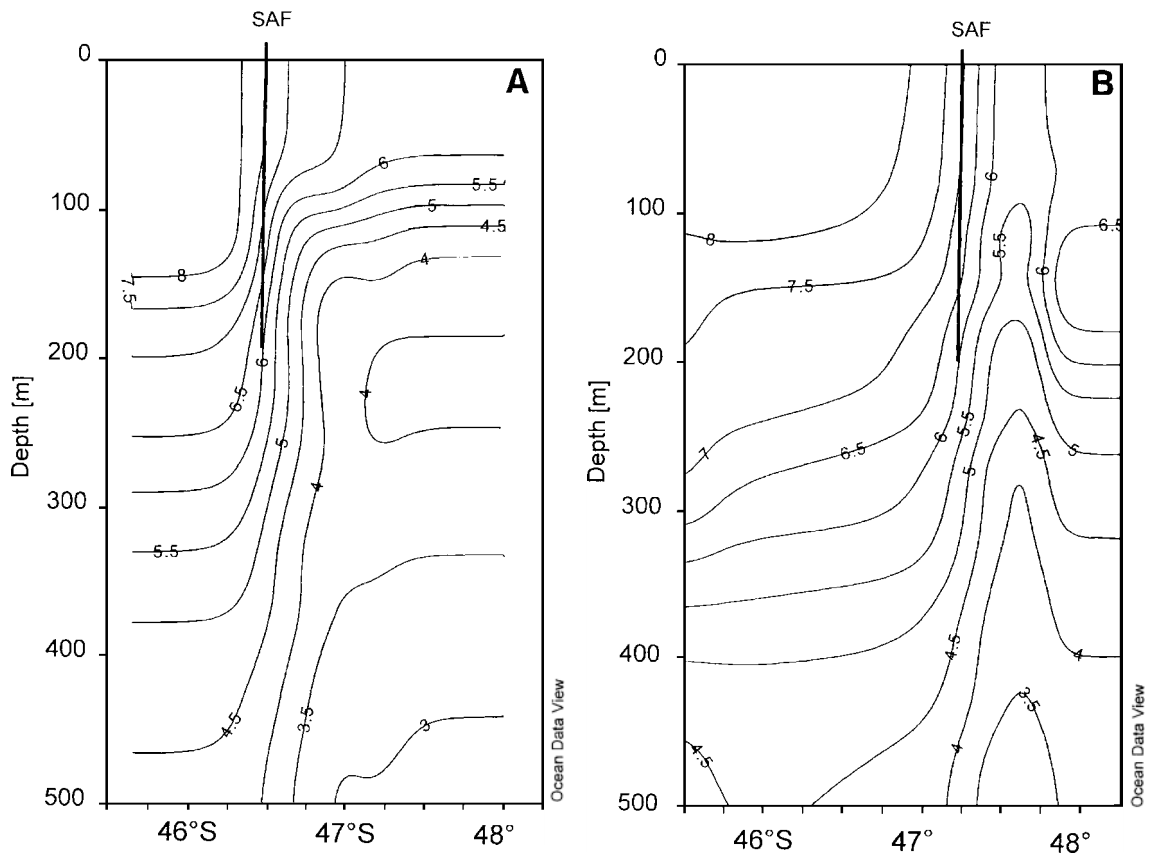

Fig. 3. Vertical temperature section (top 500 m) along 35°51′E occupied upstream of the Prince Edward Islands during (A) MOES 2 and (B) MIOS 2. The position of the SAF can be identified from the 6 °C isotherm intersection at 200 m (after Park et al., 1993).

bordering the Polar Frontal Zone (Belkin and Gordon, 1996). Depending on authors, these definitions are based on either surface or subsurface property values, whereas others have used phenomenological definitions (Park et al., 1993). Definitions for both surface and subsurface ranges are given in Table 1; however, in order to unambiguously place the fronts before describing the frontal features observed in the region surrounding the Prince Edward Islands, each front will be defined using their representative subsurface axial values at 200 m where generally each front is marked best.

We wish to compare this data set with a similar study of this region, so we shall use the definitions of Belkin and Gordon (1996) and Orsi et al. (1995) (Table 1). Consequently, for the purpose of this study, the definition used by Belkin and Gordon (1996), in which Θ/S ranges between 4.8 and 8.4 °C and 34.11–34.47 at 200 m, with axial values of 6.6 °C and 34.3 will be used to identify the SAF (Table 1). In order to define the subsurface expression of the APF, the definition given by Orsi et al. (1995), in which the axial value marks the intersection of the 2 °C isotherm at 200 m, will be used. Extensive analysis by Belkin
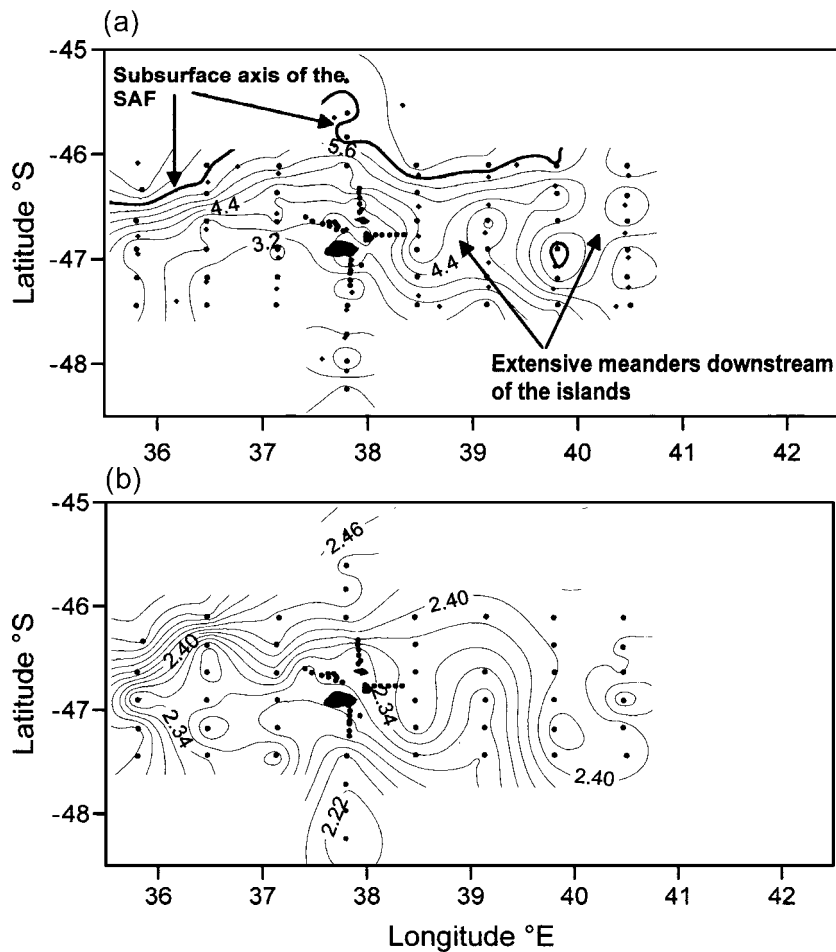

Fig. 4. Horizontal distribution of temperature (°C) at (a) 200 m and (b) 1500 m during MOES 2. Upstream of the islands, the SAF appears as a zonal band lying between temperature ranges of 6.8 and 4.4 °C at 200 m, and between 3.2 and 2.34 °C at 1500 m. The subsurface SAF axis is in bold. Downstream of the islands, an extensive meandering pattern is observed within the PFZ. Black dots represent the position of all CTD stations and diamonds for all XBT stations to a maximum depth of 760 m.

and Gordon (1996) have found the subsurface SAF and APF axial values to remain fairly stable between 0° and 150°E.

Both MOES 2 and MIOS 2 crossed from Subantarctic Surface waters (SASW) in the Subantarctic Zone north of the SAF through to waters resembling Antarctic Surface water (AASW) in the Polar Frontal Zone (PFZ). The Subantarctic Zone extends from the Subtropical Convergence to the Subantarctic Front. Deacon (1937) found the salinity in the Indian sector of the Subantarctic Zone to be between 33.8 and 34.4 and temperatures from 3 to 14 °C. SASW extends from the surface to the depth of the

Antarctic Intermediate Water and is characterised by a shallow subsurface salinity maximum as a result of excess precipitation over evaporation at these mid-latitudes.

Further south, AASW can be found separated from SASW by the APF. AASW is characterised by a shallow temperature minimum associated with the remnants of Winter Water. This water mass is seasonally variable; in winter, it is nearly homogenous extending to 250 m, while in summer, the mixed layer extends only between 50 and 100 m. Temperature ranges from − 1.8 to 6 °C at the APF and salinity from 33.4 to 34.2.
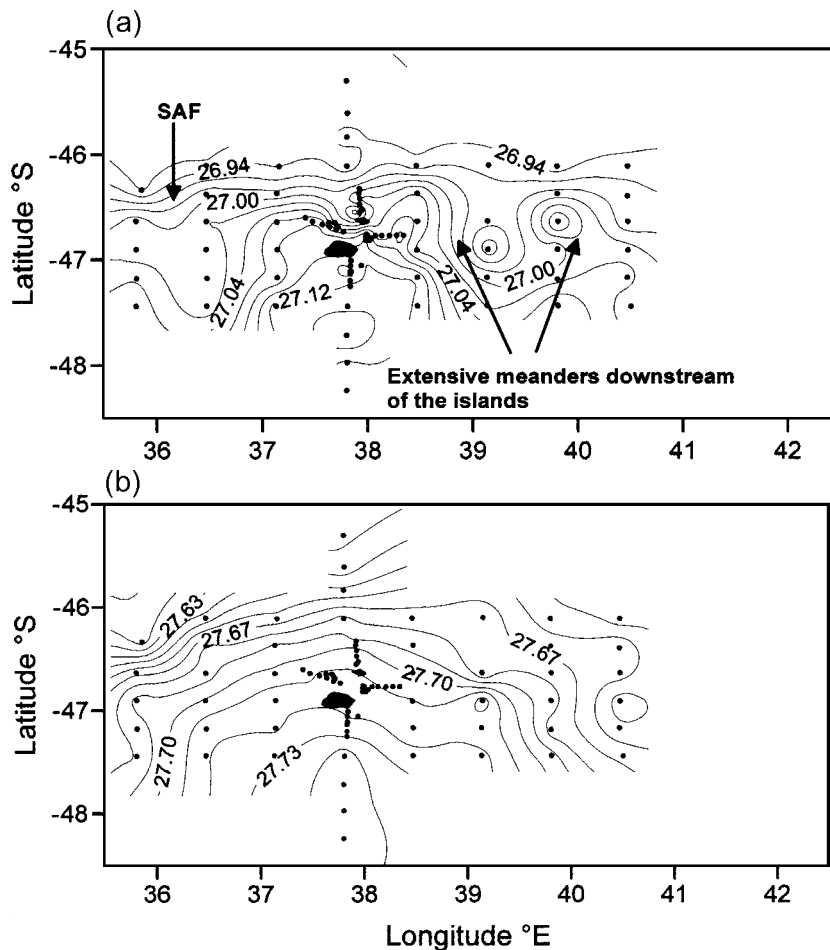

Fig. 5. Horizontal distribution of density (kg m^{-3}) at (a) 200 m and (b) 1500 m during MOES 2. Upstream of the islands, the SAF appears as a zonal band lying between density ranges of 26.92 and 27.00 kg m^{-3} at 200 m, and between 27.62 and 27.69 kg m^{-3} at 1500 m. Black dots represent the position of all CTD stations.

The PFZ is a transitional zone between SASW and AASW. Its exact boundaries can be difficult to decide due to the ephemeral nature of the SAF. As a consequence and for ease in deciding the boundaries of the PFZ, the authors have used the subsurface definitions outlined in Table 1. Consequently, the northern boundary of the PFZ is defined by the subsurface expression of the SAF (6.6 °C—200 m after Belkin and Gordon, 1996) and the southern boundary is defined by the subsurface expression of the APF (2 °C—200 m after Orsi et al., 1995).

4. Results

Results from the MOES 2 and the MIOS 2 give the first quasi-synoptic portrayals of the ocean surroundings of the islands.

During MOES 2, the SAF was observed upstream of the islands (along 35°51′ E) at 46°30′ S (Fig. 3A). Closer to the islands, its path was deflected northwards to approximately 46°S. Farther downstream, subsurface temperatures and density values gradually decreased poleward across the PFZ—between 46°S and 48°S—from 7.0 to 3.2 °C and from 26.92 to 27.10 kg m^{-3}
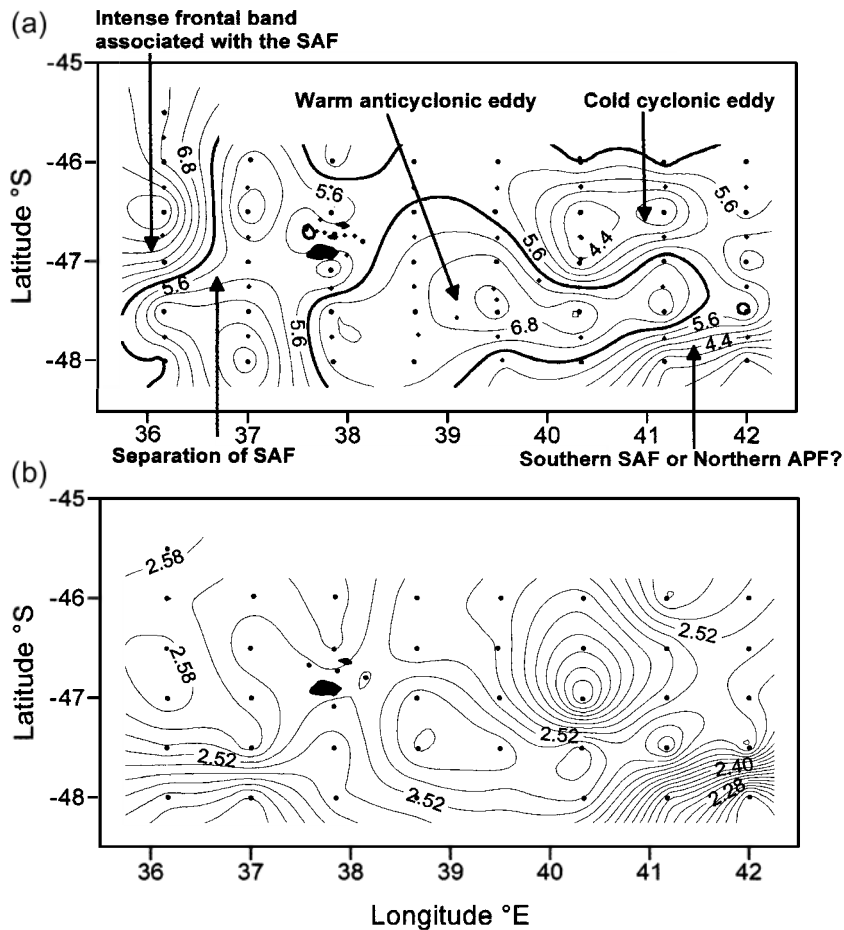

Fig. 6. Horizontal distribution of temperature (°C) at (a) 200 m and (b) 1500 m during MIOS 2. The strong frontal region associated with the SAF upstream of the islands can be clearly seen from the bunched isotherms, which range from 8.4 to 4.8 °C at 200 m, with the subsurface SAF axis in bold. Closer to the islands, the SAF separates forming a northern or southern branch. Two counter-rotating eddies, cold cyclonic to the north and a warm anticyclonic to the south, are clearly evident downstream of the islands. The sharp thermal gradients in the southeastern corner of the survey are possibly indicative of the Southern SAF or the northern boundary of the APF. Black dots represent the position of all CTD and diamonds for all XBT stations to a maximum depth of 760 m.

(Figs. 4a and 5a). These values are typical of the transitional character of the PFZ (Perissinotto et al., 2000).

Downstream, the SAF remained to the north of the survey grid and subsurface distributions of temperature and density show the existence of a distinct, broad, meandering wake with a wavelength of 120 km within the PFZ (Figs. 4a and 5a). Temperature and density distributions show this wake to be deep, extending to 1500 m (Figs. 4b and 5b). The APF was not encountered during MOES 2, although subsurface temperatures gradually decreased south of the islands to 2.4 °C at 48°15′S (CTD 19 Fig. 4a), suggesting that the APF may be lying in close proximity.

The oceanic environment surrounding the Prince Edward Islands during the MIOS 2 proved to be very different. Upstream, the SAF was found to lie much farther south, at 47°20′S, where it formed an intensive frontal feature (Fig. 3B) extending to 1500 m (Fig. 6b) Subsurface temperatures (Fig. 6a) and salinities across this front ranged from 8.0 to 4.8 °C and 34.27 to 34.1, respectively, and are in agreement with the definitions outlined by Belkin and Gordon (1996) in Table 1. Closer to the islands, the SAF separated with a single branch flowing to the north of the Prince Edward Islands, while a second branch meandered to the south (Figs. 6 and 7).
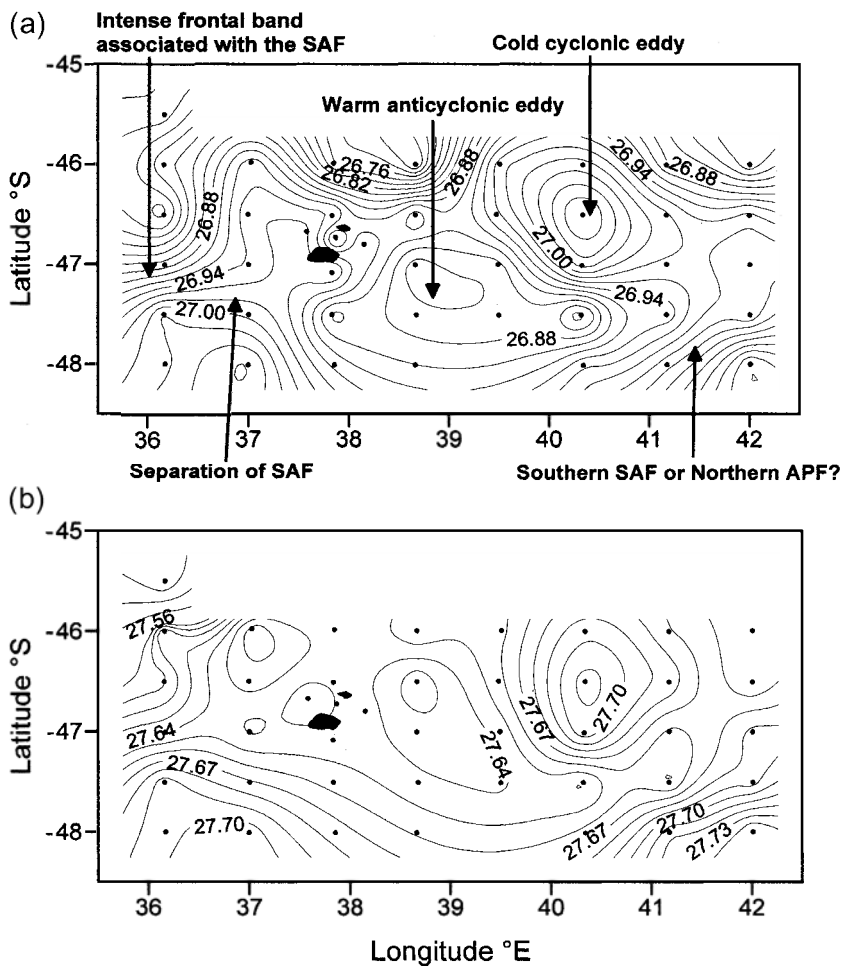

Fig. 7. Horizontal distribution of density (kg m⁻³) at (a) 200 m and (b) 1500 m during MIOS 2. The strong frontal region associated with the SAF upstream of the islands can be clearly seen from the bunched isopycnals. Black dots represent the position of all CTD stations.

Downstream of the islands, the subsurface isotherm (6 °C) and isopycnal (26.90 kg m^{-3}) representing the axis of the SAF show that the front remained north of the survey grid, possibly having been forced northwards by the existence of two counter-rotating eddies (Figs. 6a and 7a). A cold cyclonic (<5 °C, <34.1; Fig. 6a) eddy extending to 1500 m was encountered to the north (Figs. 6b and 7b), while to the south, a warm anticyclonic (>6 °C) eddy was found.

Finally, what is the front in the southeastern corner of the survey grid? Subsurface temperatures at this front range from 5.6 to 2.8 °C and are too

cold for the definition of the SAF given in Table 1. However, the 2 °C temperature minimum is also too deep for this to be considered as the APF (Fig. 13). Closer inspection suggests that this frontal feature may be the southern branch of the SAF, which having separated upstream of the islands continues to meander to the south.

The path taken by both northern and southern branches of the SAF east of the survey grid can only be speculated. However, subsurface density distributions (Fig. 7a) show a gradual merging of isopycnals at 42°E, suggesting that having "rounded" both cyclonic
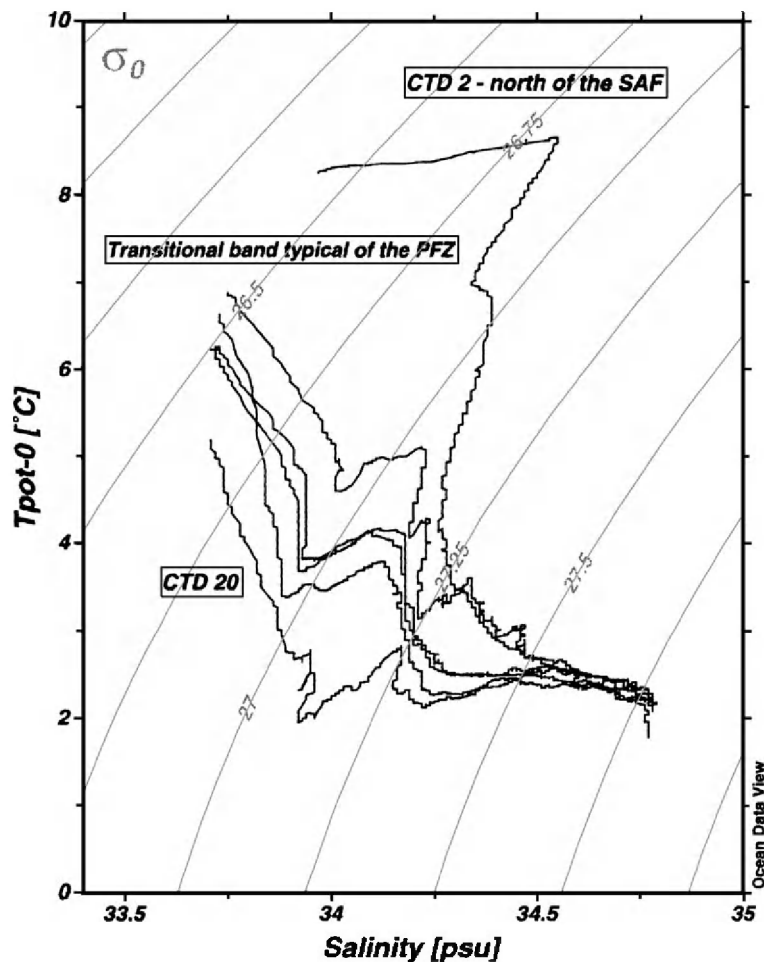

Fig. 8. Θ/S profiles for CTD stations 2–6 (35°51′E) in the upstream region during MOES 2. CTD station 2 clearly shows a profile consistent with water characteristics typical of the Subantarctic Zone (SAZ). In addition, the profile associated with CTD station 20, which lies south of the islands at 37°48′E, has also been included for comparison as this station consists of Antarctic Surface Water (AASW) typical of the Antarctic Zone (AAZ). Θ/S profiles show the gradual transition from SASW to AASW characteristic of the PFZ.

and anticyclonic eddies, the SAF may in fact merge again into a single frontal band further downstream.

5. Discussion—water masses

5.1. Upstream region—MOES 2 and MIOS 2

During MOES 2, water masses in the entire upstream region showed a gradual transition from Subantarctic Surface Water (SASW) to the waters more closely resembling Antarctic Surface Water (AASW).

Surface temperatures steadily dropped from 7.0 to 5.1 °C and salinities from 33.75 to 33.71 across the survey grid (Fig. 8). Upstream of the islands only a single station (CTD 2) lay north of the SAF subsurface axis. Its Θ/S properties were distinctly SASW, with a strong shallow salinity maximum (>34.5) at the base of the surface mixed layer.

SASW is strongly influenced by mixing with the adjacent subtropical gyres and air–sea interactions along its circumpolar path. Comparisons with hydrographic stations in the Drake Passage (Sievers and Nowlin, 1984) show that in the Indian sector of the
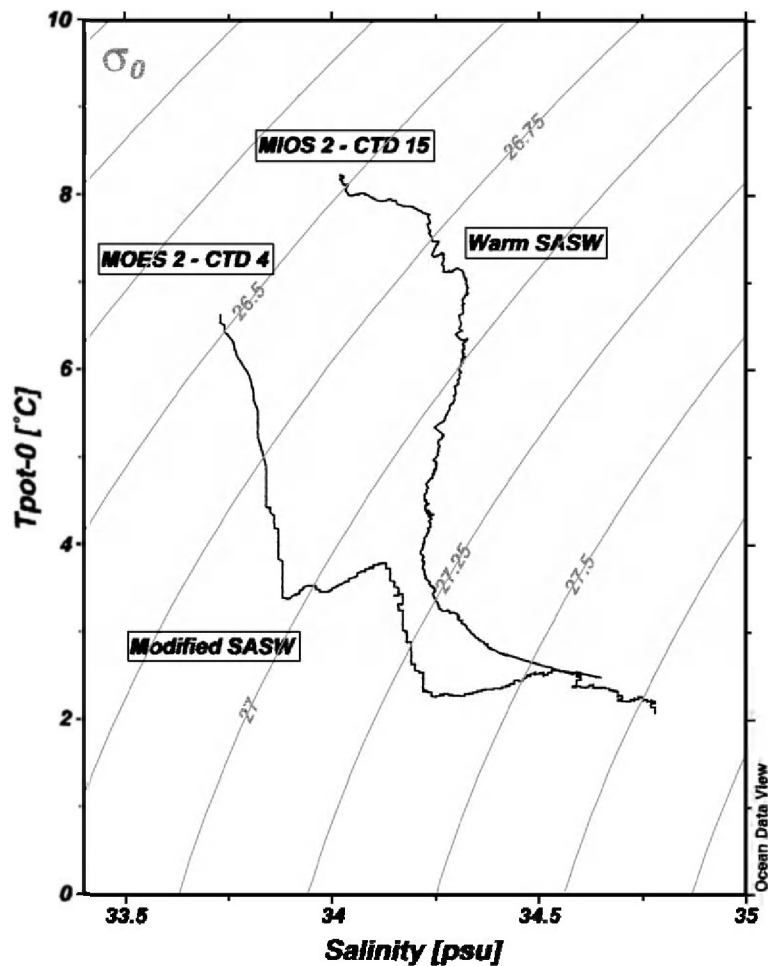

Fig. 9. A comparison between Θ/S profiles for CTD station 4 (MOES 2) and CTD station 15 (MIOS 2), which can both be found at the same location upstream of the islands. The profiles clearly show the effect the geographical position of the SAF has on the local environment. A warm, saline Θ/S profile is associated with the MIOS 2 survey during which the SAF lay farther to the south, whereas a cooler, fresher profile is associated with the MOES 2 survey during which the SAF lay farther north.

Southern Ocean, SASW is more saline (by ~ 0.02). The Agulhas Current system may also have a strong influence in this region by increasing surface temperatures and salinities (Lutjeharms and Ansorge, 2001). This may partially explain the higher values observed during this survey.

During the MIOS 2 survey, the SAF lay farther south (47°20′ S; Fig. 3B) than during previous studies (Lutjeharms and Valentine, 1984). An extremely intense temperature gradient of 0.05 °C/km was observed for the first time in this region. In comparison to MOES 2, where only a single station (Fig. 8; CTD 2) lay north of the SAF subsurface axis, during MIOS 2, the southward shift of the SAF resulted in the majority of stations occupied during the first transect (36°E) lying to the north of the SAF subsurface axis (Figs. 3B and 6a). As a consequence, the surface environment upstream of the Prince Edward Islands during MIOS 2 was warmer (by >1.5 °C) and saltier (by ~ 0.4) (Fig. 9).
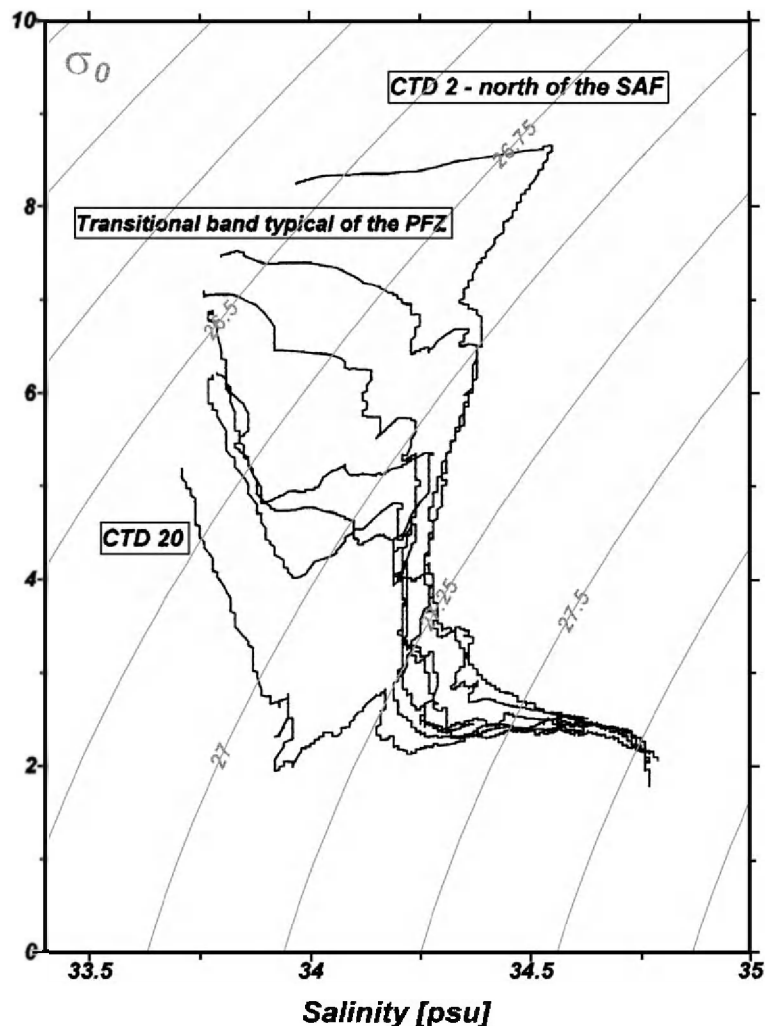

Fig. 10. Θ/S profiles for CTD stations 54–58 during MOES 2. This transect was located within the poleward excursion of the downstream wake. Profiles show the southward advection of SASW (7.5–6 °C; ~ 33.8) from north of the SAF. In addition, CTD stations 2 and 20, which come from different sections, have been included as they illustrate the full range of water properties encountered during MOES 2.

5.2. Downstream region—MOES 2

Downstream of the Prince Edward Islands, the subsurface properties of the SAF demonstrated a distinct wake between 38°30′ E and 40°30′ E (Fig. 4a and b). Deacon (1983) has postulated that the complexity of the current regime in the vicinity of the islands results in an increase in the interchange of Antarctic and Subantarctic Surface water within the PFZ. In fact,

the subsurface waters associated with CTD 54–58, the westernmost transect in the downstream region, are warmer (by ∼ 1 °C) and more saline (by +0.05) than those of stations located upstream. Subsurface temperatures across the downstream survey area ranged meridionally from 6.6 to 3.0 °C compared to 7.0 to 3.8 °C upstream. The difference in temperature range is largely due to the meandering dynamics of the SAF seen downstream of the Prince Edward Islands, sug-
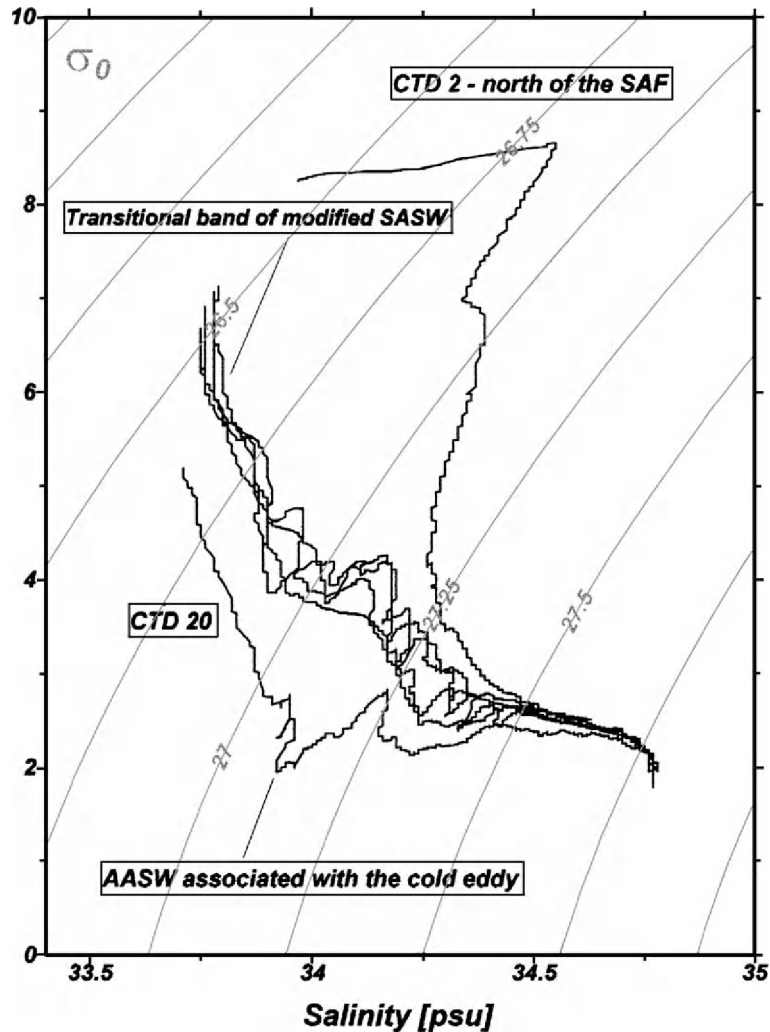

Fig. 11. Θ/S profiles for CTD stations 60 and 65 during MOES 2. This transect was located in the equatorward excursion of the downstream meander and therefore in the region where cooler, modified SASW was advected northwards across the PFZ. CTD station 2 (SAZ) and CTD station 20 (AAZ) represent stations located outside the Polar Frontal Zone (PFZ) and are used to illustrate the full range of water properties encountered during MOES 2.

gesting that distinctly warm (>5 °C) SASW may have been advected southwards into the PFZ (Fig. 10). Despite this increase in temperature, the gradual modification of this water mass with distance across the PFZ is still apparent.

In contrast, CTD 60–64, which lay on the equatorward, leading edge of the wake, were in water that was cooler (4.2 °C) and fresher (33.9) than the previous transect, as modified AASW was advected farther northwards (Fig. 11). Subsurface salinities varied by 0.30 between the two transects (CTD 54–59 and CTD

60–64) and further emphasise the influence meanders within the PFZ have on modifying this ocean environment.

5.3. Downstream region—MIOS 2

During MIOS 2, the subsurface expression of the SAF at 46°15′S appeared to flow parallel to the deep (>2500 m) channel separating the Gallieni Rise and the Del Cano Rise. This is comparable with recent findings by Pollard and Read (2001), who were able
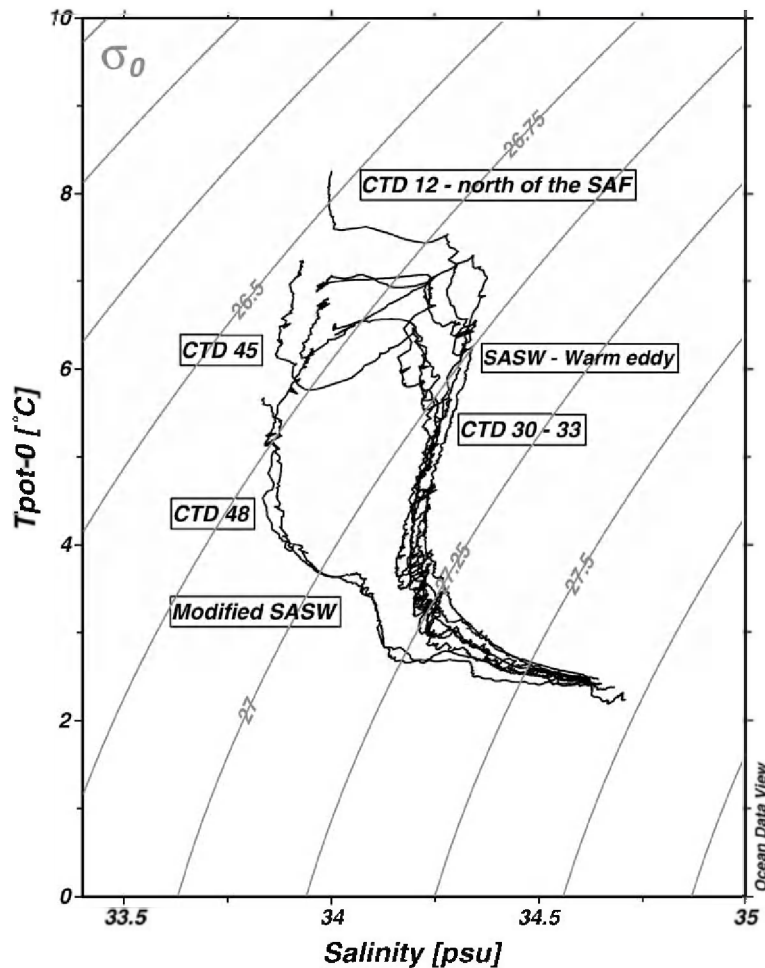

Fig. 12. Θ/S profiles for CTD stations 30–33 and 54 during MIOS 2. This transect was located immediately downstream of the islands during MIOS 2 and passes through a warm eddy. The Θ/S characteristics shown are typical of warm SASW, suggesting that the eddy may have been spawned from the SAF. For comparison, CTD station 45 has been included, as it is located within a cold eddy and its profile is indicative of AASW. CTD station 12 (SAZ) and CTD station 48 (AFZ) represent stations located outside the Polar Frontal Zone (PFZ) and are included for comparison.

to show from a series of current meters deployed during the research programme SWINDEX, that the major part of the transport of the ACC, 80–90Sv, passes south of the Del Cano Rise. In contrast, south of the islands where the topography falls off rapidly to form the deep (>4000 m) Enderby abyssal plain, the Southern SAF exists as a meandering flow seemingly unaffected by local bathymetry. Separating the two frontal bands downstream of the islands during MIOS 2 were two counter-rotating eddies within the PFZ.

5.4. Cold eddy

Θ/S profiles suggest this cold eddy consisted of modified AASW (<6 °C, <33.9), which had been advected northwards and trapped in the PFZ. The Θ/S curve associated with CTD 45, located in the core of the eddy, is almost identical to that of CTD 48, which lay on the southeastern boundary of the survey grid (Fig. 12). Koshlyakov et al. (1985) have shown that Subantarctic water masses may become entrained by the cyclonic rotation of cold eddies in the PFZ. Indeed, the Θ/S curve of water in the eddy shows a slight increase in subsurface temperatures and salinities at 27.10 kg m^{-3}, characteristic of SASW. This observation of entrainment of ambient waters by eddies is also consistent with hydrographic studies on cyclonic rings carried out in the Gulf Stream (Richardson, 1981) and in the Kuroshio Current (Kawai, 1972).

The position of this eddy may have acted as a distinct hindrance to the baroclinic flow associated with the SAF, forcing it to remain north of the survey grid. This observation is consistent with that of Sievers and Emery (1978), who have shown that when a separate cold feature occupied the PFZ, the SAF intensified and moved northwards resulting in a widening of the PFZ. It is possible that this eddy may have been quasi-stationary, its position possibly influenced by the shallow Africana Rise which lies immediately northeast (Fig. 1). Past hydrological investigations by Koshlyakov et al. (1985) and satellite observations by Gouretski and Danilov (1994) have indicated similar features in the same region on a number of occasions.

Hofmann and Whitworth (1985) have described a cold eddy that remained in the Drake Passage for over 20 weeks, suggesting that its eastward progress may have been hampered by the bathymetry. Although we

do not have direct observations for the persistence of the cold eddy observed during MIOS 2, it is likely that the irregular topography associated with the Africana and Del Cano Rise could have affected its subsequent eastward passage.

In the southeastern corner of the survey grid, sharp horizontal gradients in both subsurface temperature and density (5.6–2.8 °C and 26.98–27.14 kg m^{-3}) (Figs. 6a and 7a) agree with Holliday and Read (1998) and are indicative of the meandering Southern SAF. However, a vertical section through this feature (Fig.

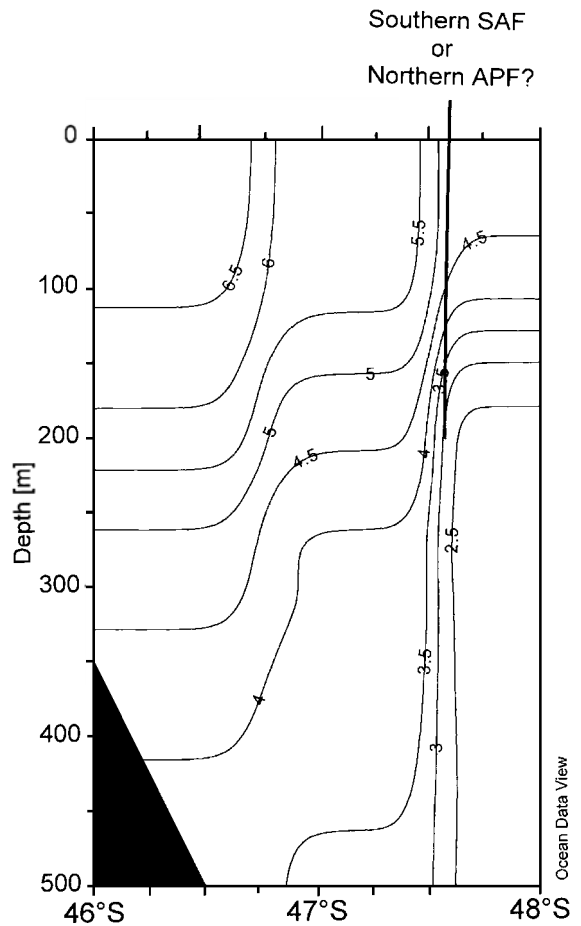Fig. 13. Vertical temperature section (top 500 m) along 42°E during the MIOS 2 survey. A strong frontal band can be found at 47°30′S. It is not clear whether this front represents the southern branch of the SAF or the northern boundary of the APF. Temperatures at 200 m are 3 °C, which although too warm to satisfy the criteria for the APF outlined in Table 1, are also too cold to represent the SAF proper.

I.J. Ansorge, J.R.E. Lutjeharms / Journal of Marine Systems 37 (2002) 107–127

13) shows the location of the 3 °C isotherm at 200 m. This does not fit the definition for the subsurface APF given in Table 1; however, it does suggest that the APF may have been in close proximity to the southeastern corner of the survey grid. Further support is also given by the Θ/S properties associated with CTD 49; typically, AASW with a near surface temperature minimum at 27.10 kg m^{-3} associated with the remnants of Winter Water.

5.5. Warm eddy

A warm (>6 °C), elongated eddy was encountered south of the cold eddy. Horizontal subsurface distributions of temperature and density (Figs. 6a and 7a) show this feature to extend the length of the survey
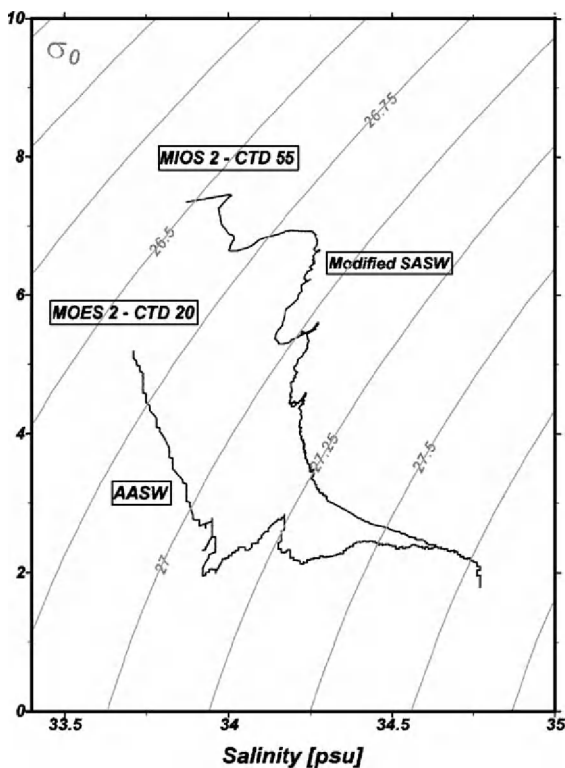

Fig. 14. Θ/S profiles showing the difference in water characteristics between stations located immediately south of the islands during the two surveys. The profile associated with CTD station 20 (MOES 2) is characteristically AASW hinting at the close proximity of the APF. In contrast, CTD station 55—occupied during MIOS 2—is characteristic of SASW that has been entrapped into the region by a warm eddy.

grid. A subsurface salinity maximum (34.25) in the Θ/S curves confirm the presence of SASW in this warm feature. Indeed, the warm (>6 °C), saline (>33.9) characteristics of this feature are similar to that of CTD 12, which lay far north of the SAF in the upstream region of the islands (Fig. 12).

Sections through the eddy (not shown) indicate a deep mixed layer of 150–200 m. Perissinotto et al. (2000) have shown that these mesoscale disturbances have a major impact on modifying the vertical stability of the water column and the depth of the mixed layer in this region. The formation of this eddy may have resulted from the breakdown of a wake, similar to that observed during MOES 2. Observations in the Drake Passage by Joyce and Patterson (1977) have shown that instabilities generated in a meander at the border of the PFZ are primarily responsible for its final collapse, resulting in the formation of mesoscale eddies within the PFZ.

The substantial differences observed in the Θ/S curves between repeat stations south of the Prince Edward Islands highlights the variability of the oceanic environment here. During MOES 2, the existence of a cold feature south of the islands (Fig. 4—CTD 20), possibly spawned from the APF, resulted in Θ/S curves typical of AASW. In this region, surface temperatures range from 3.0 to 5.0 °C and a temperature minimum (2 °C) associated with Winter Water typical of AASW was observed at 27.10 kg m^{-3}. In contrast, during MIOS 2 (at the same location—CTD 55), the existence of a warm eddy resulted in Θ/S curves indicative of the southward advection of SASW (Fig. 14). Here a shallow subsurface salinity maximum (34.3) can be seen at 26.90 kg m^{-3}. In addition, a salinity minimum (34.2) at 27.25 kg m^{-3} is typical of Antarctic Intermediate Water, which has formed as a result of AASW sinking at the APF (Deacon, 1937).

6. Discussion—geostrophic velocities

Geostrophic flow has been calculated using a Matlab sw_vel.mfile obtained from SEAMAT between station pairs at every 1 db pressure level to a maximum reference depth of 1500 db. Technical problems with the spooling of the hydrographic wire prevented the CTD instrument from being lowered below 2000 m. Since the Antarctic Circumpolar Current is known to

extend to depths exceeding this (e.g. Nowlin et al., 1977), the following speed calculations are likely to be underestimates.

6.1. MOES 2

Upstream of the islands the high-speed core associated with the SAF axis was found to lie along the northern edge of the survey, between 46° and 46°38′ S, with geostrophic velocities between station pairs ranging from 20 to 28 cm s^{-1} (Fig. 15). Geostrophic velocities dramatically decreased (<5 cm s^{-1}) immediately south of the SAF subsurface axis. Relatively quiescent zones separate the SAF and APF and therefore velocities associated with the PFZ are usually minor (Nowlin et al., 1977).

Topographical steering by the Prince Edward Islands may have resulted in the SAF deflecting northeastwards to lie between CTD 50 and 52, with speeds exceeding 23 cm s^{-1}. There was a substantial reduction in speeds immediately north of CTD 52 (0.54 cm s^{-1}) and south of CTD 50 (7 cm s^{-1}) indicating that the SAF lay in a narrow concentrated band, only 55 km wide. Recent investigations by Pollard and Read (2001) during SWINDEX have shown that between the gap west of Crozet and the Del Cano Rise, the ACC, influenced by the shallow and com-

plex regional topography, narrows to between 40 and 70 km. Alternating eastward and westward flows south of the islands are associated with the cyclonic motion of a cold eddy possibly spawned from the APF (Figs. 4 and 15).

Downstream, geostrophic velocities show strong (>16 cm s^{-1}) alternating westward and eastward flows around pools of weaker currents (5 cm s^{-1}) indicative of a meander within the PFZ. Comparing hydrographic data with vectors generated using the Fine Resolution Antarctic Model (FRAM) for the region north of South Georgia, Trathan et al. (1997) have shown that in the centre of a high speed meander lay relatively still waters (<3 cm s^{-1}), which were stable and well mixed. Indeed, stations located in the warm eddy of the MIOS 2 have well-developed mixed layers with depths extending to >60 m (Perissinotto et al., 2000).

The highest velocities >30 cm s^{-1} observed during the entire survey were found along transect 6 (CTD 64–63), where the flow associated with the equatorward leading branch of the meander was coupled with the strong zonal flow associated with the SAF. Farther downstream a westward current (>9 cm s^{-1}), a component of the anticyclonic motion of the warm eddy between CTD 73 and 74 was observed (Fig. 15). We are unable to determine the extent of the wake
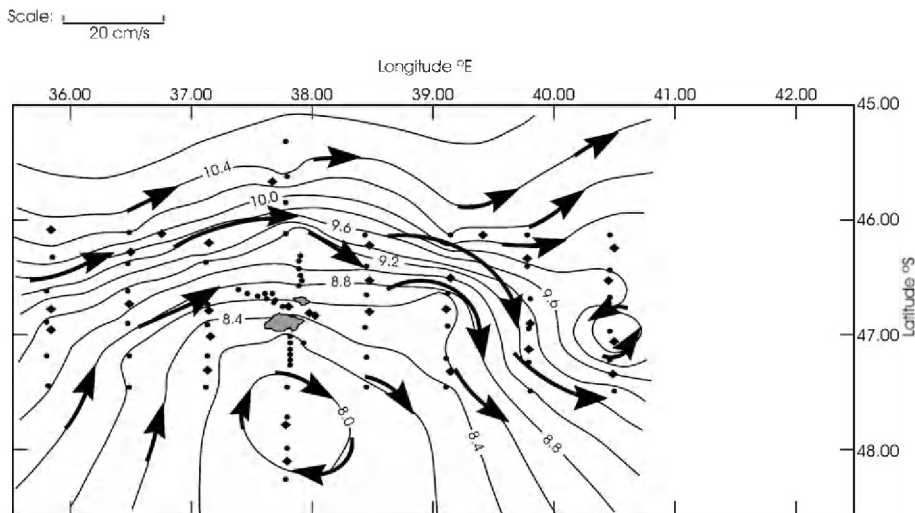

Fig. 15. Dynamic height (at 0 db referenced to 1500 db) during MOES 2. Arrows indicating the surface geostrophic velocities have been superimposed onto the dynamic height and reflect the velocities calculated between stations. The meandering nature of the SAF can be clearly seen, as well as the position of a cold cyclonic eddy immediately south of the islands and a warm anticyclonic eddy downstream.

downstream of the survey grid. However, laboratory experiments in which the interaction of linear Rossby waves with nonzonal ridges was studied (Roden, 1991) have shown that the amplitudes of such a wake decrease exponentially with distance from the ridge. This agrees with field studies around the island of Oahu, which have shown a Rossby wave breaking down 250 km downstream of a ridge (Mysak and Magaard, 1983). The wake observed at the Prince Edward Islands during the MOES 2—if indeed a true Rossby wave—could therefore have extended considerably farther than the station grid.

6.2. MIOS 2

In comparison to the MOES 2, where the SAF lay as a zonal band (upstream of the islands) between $46°$ S and $46°38'$ S, during the MIOS 2 following its separation, the northern branch of the SAF appeared to meander extensively from where it initially lay far to the south at $47°20'$ S (CTD 15–16). The two transects, occupied upstream of the islands (CTD 12–22) both show alternating eastward and westward flow indicative of a meandering front. The meandering nature of the northern branch of the SAF in this region may have been due to the presence of a cold eddy centred at $46°30'$ S, $37°$ E, causing the SAF to deflect northwards.

Geostrophic velocities show this eddy to have been cyclonic with speeds ranging between 5 and 9 cm s^{-1}. Maximum speeds (>25 cm s^{-1}) encountered during the upstream transects were associated with the intense SAF frontal band found between CTD 14 and 16. Closer to the islands, the SAF appeared to branch, reducing speeds substantially to 11 cm s^{-1} (northern branch—CTD 19–20) and 12 cm s^{-1} (southern branch—CTD 18–19).

The general circulation downstream of the islands was dominated by two counter-rotating eddies (Fig. 16). Geostrophic velocities along the northern edge of the grid were high (>15 cm s^{-1}) and are in agreement with the hydrography, which suggests that the Northern SAF lay on the edge of the survey grid, having been displaced northwards by the cold eddy.

Immediately east of the islands and south of the northern branch of the SAF, geostrophic velocities had both westward (9 cm s^{-1}) and eastward (6 cm s^{-1}) components associated with the anticyclonic motion of a warm eddy. In the centre of this eddy (CTD 30 and 31), flow was extremely weak (>1 cm s^{-1}).

In the northeastern corner of the survey grid, the general geostrophic flow associated with the cold eddy was cyclonic. Similar to MOES 2, there was an increase in flow to 16 cm s^{-1} (CTD 44–46), as the cyclonic flow appeared to couple with the northern branch of the SAF. The strongest surface flow >30 cm
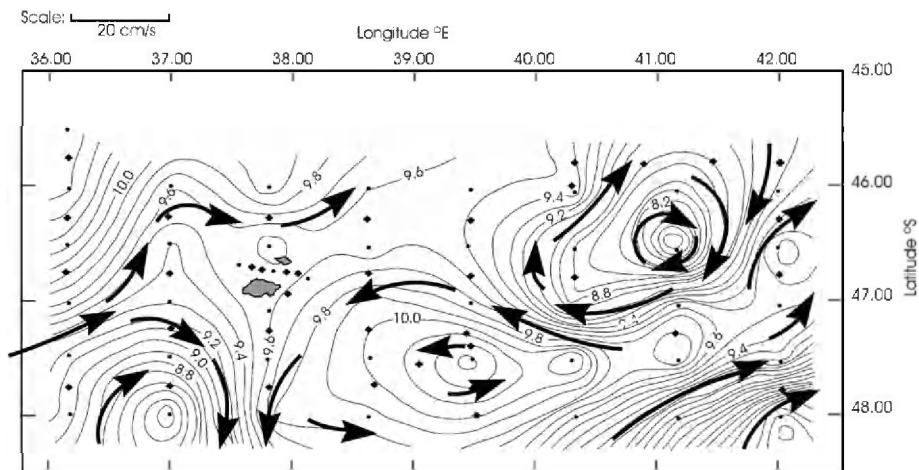

Fig. 16. Dynamic height (at 0 db referenced to 1500 db) during MIOS 2. Arrows indicating the surface geostrophic velocities have been superimposed onto the dynamic height and reflect the velocities calculated between stations. The branching of the SAF frontal band upstream of the islands can be clearly seen. Downstream of the islands, the cyclonic flow associated with a cold eddy as well as the anticyclonic motion of a warm eddy are evident.

s^{-1} observed in the whole survey was found between CTD 40 and 41 and was associated with the coupling between the warm and cold eddy (Fig. 16). Here a strong thermal gradient (0.03 °C/km) extended through the water column. In the southeastern corner of the survey grid, the southern branch of the SAF was encountered again and here speeds exceeded 24 cm s^{-1}.

Both surveys demonstrate that the flow regime downstream of the Prince Edward Islands is complex and dynamic. Investigations elsewhere (e.g. Barkley, 1972; Heywood et al., 1990) have all shown that the size and form of flow disturbances, such as trapped eddies and meandering wakes, downstream of islands are directly related to the velocity at which the incident current reaches the islands. Observations during the MOES 2 and the MIOS 2 are consistent with this concept. At higher incident speeds of the ACC (MOES 2), a meandering wake was observed to extend the length of the survey grid downstream of the islands, while during a period of less intense flow as a result of the separation of the SAF during MIOS 2, two counter-rotating eddies with no identifiable wake were observed. Under both conditions, the displacement of the SAF was apparent (Ansorge et al., 1999; Froneman et al., 1999), resulting in the advection across and entrapment of water masses within the PFZ.

7. Conclusions

Previous results based on satellite observations (Colton and Chase, 1983), buoy trajectories (Hofmann, 1985), inertial jet models (Craneguy and Park, 1999) and hydrographic data (e.g. Lutjeharms and Baker, 1980; Park et al., 1993; Trathan et al., 1997) have all revealed that high mesoscale variability in the Southern Ocean is closely correlated with regions of prominent bottom relief. The Prince Edward Islands lie in such a region, bordered to the west by the shallow Southwest Indian Ridge, while to the east and north lie the Del Cano Rise and the Gallieni Rise.

Furthermore, extensive surveys throughout the Southern Ocean, such as those at Crozet and Kerguelen (Park et al., 1991, 1993) and South Georgia (Atkinson and Peck, 1990; Trathan et al., 1997), have

all revealed extensive mesoscale disturbances within the PFZ in the vicinity of islands.

The MOES 2 and MIOS 2 surveys both show the deflection of the SAF around the northern edge of the Prince Edward Islands. However, comparisons between the results of the two surveys show that the flow patterns in the downstream region varied substantially with a meandering wake during MOES 2 and two counter-rotating eddies during MIOS 2.

The meandering motion of the SAF during MOES 2 resulted in the southward displacement of water masses from the north, while the warm and cold eddies featured in MIOS 2 appeared to be less motile, trapping AASW and SASW within the PFZ. The results show that during both occasions, the leeward side of the Prince Edward Islands represented a region of enhanced meridional exchange of water masses, probably resulting from the interaction between the complex bottom topography and the eastward flowing ACC.

Whether the Prince Edward islands create their own disturbance downstream or whether they lie at the tail end of a region of enhanced variability (Park and Gamberoni, 1995) still remains unresolved. The position of the islands directly in the path of the ACC could certainly play a role in changing the pattern of the flow. But how great a role is it?

Extensive research has indicated that both the SAF and the APF are characterised by the genesis of eddies. Such spin-off eddies may subsequently be advected into the island vicinity (Lutjeharms and Baker, 1980; Gouretski and Danilov, 1994; Moore et al., 1999).

To understand the impact the Prince Edward Islands may have on the position of the SAF, the region upstream between the Prince Edward Islands and the Southwest Indian Ridge needs to be further explored. A proposal to extend the MOES/MIOS-type survey upstream of the islands has been accepted and a cruise planned for April 2002. The aim would be to follow the advection of mesoscale features from upstream to the island vicinity.

Agulhas for their hard work during each voyage. We would also like to acknowledge the constructive criticism of three anonymous reviewers.

References

Allanson, B.R., Boden, B.P., Parker, L.D., Duncombe Rae, C.M., 1985. A contribution to the oceanology of the Prince Edward Islands. In: Siegfried, W.R., Condy, P.R., Laws, R.M. (Eds.), Antarctic Nutrient Cycles and Food Webs. Springer, Berlin, pp. 30–45.

Ansorge, I.J., Froneman, P.W., Pakhomov, E.P., Lutjeharms, J.R.E., 1998. Hydrographic Data Report on the Marion Island Oceanographic Survey 2 (MIOS2). UCT Oceanographic Report 98-1.

Ansorge, I.J., Froneman, P.W., Pakhomov, E.P., Lutjeharms, J.R.E., Perissinotto, R., Van Ballegooyen, R.C., 1999. Physical–biological coupling in the waters surrounding the Prince Edward Islands (Southern Ocean). Polar Biol. 21, 135–145.

Atkinson, A., Peck, J.M., 1990. The distribution of zooplankton in relation to the South Georgia shelf in summer and winter. In: Kerry, K.R., Hempel, G. (Eds.), Antarctic Ecosystems, Ecological Change and Conservation. Springer-Verlag, Heidelberg, pp. 159–165.

Barkley, R.A., 1972. Johnston atoll's wake. J. Mar. Res. 30, 201–216.

Belkin, I.M., Gordon, A.L., 1996. Southern Ocean fronts from the Greenwich meridian to Tasmania. J. Geophys. Res. 101, 3675–3696.

Boden, B.P., 1988. Observations of an island mass effect in the Prince Edward Archipelago. Polar Biol. 9, 1–8.

Boden, B.P., Parker, L.D., 1986. The plankton of the Prince Edward Islands. Polar Biol. 5, 81–93.

Colton, M.T., Chase, R.R.P., 1983. Interaction of the Antarctic Circumpolar Current with bottom topography: an investigation using satellite altimetry. J. Geophys. Res. 88, 1825–1843.

Craneguy, P., Park, Y.-H., 1999. Topographic control of the Antarctic Circumpolar Current in the South Indian Ocean. C. R. Acad. Sci. Paris 328, 583–589.

Crawford, A.B., 1972. Sea Surface Temperature Measurements by Direct Sampling Maritime Weather Office, Youngsfield, Cape Town, South Africa. 8 pp.

Deacon, G.E.R., 1937. The hydrology of the Southern Ocean. Discov. Rep. 15, 1–124.

Deacon, G.E.R., 1983. Physical and biological zonation in the Southern Ocean. Deep-Sea Res. 29, 1–15.

Duncombe Rae, C.M., 1989a. Frontal systems encountered between Southern Africa and the Prince Edwards Islands during April/May 1987. S. Afr. J. Antarct. Res. 19, 21–25.

Duncombe Rae, C.M., 1989b. Physical and chemical marine environment of the Prince Edward Islands (Southern Ocean) during April/May 1987. S. Afr. J. Mar. Sci. 8, 301–311.

Froneman, P.W., Ansorge, I.J., Pakhomov, E.P., Lutjeharms, J.R.E., 1999. Plankton community structure in the physical environ-

ment surrounding the Prince Edward Islands (Southern Ocean). Polar Biol. 22, 145–155.

Gouretski, V.V., Danilov, A.I., 1994. Characteristics of warm rings in the African sector of the Antarctic Circumpolar Current. Deep-Sea Res. 41, 1131–1157.

Heywood, K.J., Barton, E.D., Simpson, J.H., 1990. The effects of flow disturbance by an oceanic island. J. Mar. Res. 48, 55–73.

Hofmann, E.E., 1985. The large-scale horizontal structure of the Antarctic Circumpolar Current from FGGE drifters. J. Geophys. Res. 90, 7087–7097.

Hofmann, E.E., Whitworth, T., 1985. A synoptic description of the flow at the Drake Passage from year long measurements. J. Geophys. Res. 90, 7177–7187.

Holliday, N.P., Read, J.F., 1998. Surface oceanic fronts between Africa and Antarctica. Deep-Sea Res. 45, 217–238.

Joyce, T.M., Patterson, S.L., 1977. Cyclonic ring formation at the polar front in the Drake Passage. Nature 265, 131–133.

Kawai, H., 1972. Hydrography of the Kuroshio extension. In: Stommel, H., Yoshuda, K. (Eds.), Kuroshio: Physical Aspects of the Japan Current. University of Washington Press, Seattle, pp. 235–352.

Koshlyakov, M.N., Grachev, Yu.M., Sazhina, T.G., Yaremchuk, M.I., 1985. A cyclonic eddy in the Antarctic Circumpolar Current and heat transfer across the Antarctic Front. Okeanologiya/Oceanology (Moscow) 25 (6), 885–893.

Lutjeharms, J.R.E., 1990. Temperatuurstruktuur van die oseaanbolaag tussen Kaapstad en Marion-eiland. S. Afr. J. Antarct. Res. 20, 21–32.

Lutjeharms, J.R.E., Ansorge, I.J., 2001. The Agulhas Return Current. J. Mar. Syst. 30, 115–138.

Lutjeharms, J.R.E., Baker, D.J., 1980. A statistical analysis of the meso-scale dynamics of the Southern Ocean. Deep-Sea Res. 27, 145–159.

Lutjeharms, J.R.E., Valentine, H.R., 1984. Southern Ocean thermal fronts south of Africa. J. Phys. Oceanogr. 18, 761–774.

McDougal, I., 1971. . Marion and Prince Edward Islands: Report on the South African biological and Geological Expeditions, 1965–1966. Balkema, Cape Town, pp. 72–77.

Miller, D.G.M., 1982. Results of a combined hydroacoustic and midwater trawling survey of the Prince Edward Islands group. S. Afr. J. Antarct. Res. 12, 3–10.

Miller, D.G.M., Boden, B.P., Parker, L., 1984. Hydrology and bio-oceanography of the Prince Edward Islands. S. Afr. J. Antarct. Res. 14, 29–32.

Moore, J.K., Abbott, M.R., Richman, J.G., 1999. Location and dynamics of the Antarctic Polar Front from satellite sea surface temperature data. J. Geophys. Res. 104, 3059–3073.

Mysak, L.A., Magaard, L., 1983. Rossby wave driven Eulerian mean flows along nonzonal barriers, with application to the Hawaiian Ridge. J. Phys. Oceanogr. 13, 1716–1725.

Nowlin, W.D., Whitworth, T., Pillsbury, R.B., 1977. Structure and transport of the Antarctic Circumpolar Current at the Drake Passage from short-term measurements. J. Phys. Oceanogr. 7, 788–802.

Orsi, A.H., Nowlin, W.D., Whitworth, T., 1995. On the circulation and stratification of the Weddell Gyre. Deep-Sea Res., Part 1 40, 169–203.

Pakhomov, E.A., Ansorge, I.J., Froneman, P.W., 2000. Short term variability in the inter-island environment of the Prince Edward Islands. Polar Biol. 23 (9), 593–603.

Park, Y.-H., Gamberoni, E., 1995. Large-scale circulation and its variability in the South Indian Ocean from TOPEX/POSEIDON altimetry. J. Geophys. Res. 100, 24911–24929.

Park, Y.-H., Gamberoni, L., Charriaud, E., 1991. Frontal structure and transport of the Antarctic Circumpolar Current in the South Indian Ocean sector, 40–80°E. Mar. Chem. 35, 45–62.

Park, Y.-H., Gamberoni, L., Charriaud, E., 1993. Frontal structure, water masses and circulation in the Crozet Basin. J. Geophys. Res. 98, 12361–12385.

Perissinotto, R., Boden, B.P., 1989. Zooplankton–phytoplankton relationships at the Prince Edward Islands during April/May 1985 and 1986. S. Afr. J. Antarct. Res. 19, 26–30.

Perissinotto, R., Duncombe Rae, C.M., 1990. Occurrence of anti-cyclonic eddies on the Prince Edward Plateau (Southern Ocean): effects on phytoplankton biomass and production. Deep-Sea Res. 37, 777–793.

Perissinotto, R., Lutjeharms, J.R.E., Van Ballegooyen, R.C., 2000. Biological–physical interactions determining the phytoplankton productivity in the vicinity of the Prince Edward Islands, South-ern Ocean. J. Mar. Syst. 24, 327–341.

Pollard, R.T., Read, J.F., 2001. Circulation pathways and transports of the Southern Ocean in the vicinity of the Southwest Indian Ridge. J. Geophys. Res. 106, 2881–2898.

Read, J.F., Pollard, R.T., 1993. Structure and transport of the Ant-arctic Circumpolar Current and the Agulhas Return Current at 40°E. J. Geophys. Res. 98, 12281–12295.

Richardson, P.L., 1981. Gulf stream trajectories measured with drifting buoys. J. Phys. Oceanogr. 11, 888–1010.

Roden, G.I., 1991. Effects of the Hawaiian Ridge upon oceanic flow and thermohaline structure. Deep-Sea Res. 38, S623–S654.

Sievers, H.A., Emery, W.J., 1978. Variability of the Antarctic Polar Frontal Zone in the Drake Passage—summer 1976–1977. J. Geophys. Res. 83, 3010–3022.

Sievers, H.A., Nowlin, W.D., 1984. The stratification and water masses at the Drake Passage. J. Geophys. Res. 98, 14423–14435.

Sparrow, M.D., Heywood, K.J., Brown, J., Stevens, D.P., 1995. Current structure of the South Indian Ocean. J. Geophys. Res. 102, 5513–5530.

Trathan, P.N., Brandon, M.A., Murphy, E.J., 1997. Characterisation of the Antarctic Polar Frontal Zone to the north of South Geor-gia in summer 1994. J. Geophys. Res. 102, 10483–10497.

Van Ballegooyen, R.C., Perissinotto, R., Ismail, A., Boden, B.R., Lucas, M., Allanson, B.R., Lutjeharms, J.R.E., 1990. Data re-port of the second cruise of the Marion Offshore Ecological Study (MOES-II). CSIR Report EMA-D 8910, 398 pp.